Title
IAOS Bulletin 39

Permalink
https://escholarship.org/uc/item/3q96609n

Author
Dillian, Carolyn D., cdillian@coastal.edu

Publication Date
2008-06-15

IAOS

International Association for Obsidian Studies

Bulletin

CONTENTS

NEWS AND INFORMATION

CALL FOR NOMINATIONS

It's time for elections for IAOS President. Deadline for nominations is November 1, 2008. Nominations may be sent via email to current IAOS President, Anastasia Steffen at asteffen@unm.edu.

CONSIDER PUBLISHING IN THE IAOS *BULLETIN*

The *Bulletin* is a twice-yearly publication that reaches a wide audience in the obsidian community. Please review your research notes and consider submitting an article, research update, or lab report for publication in the IAOS B*ulletin*. Articles and inquiries can be sent to cdillian@princeton.edu Thank you for your help and support!

DELPHI, GREECE, OBSIDIAN CONFERENCE: January 11-14, 2008
The Dating and Provenance of Natural and Manufactured Glasses

Ioannis Liritzis, Laboratory of Archaeometry, Dept. of Mediterranean Studies, University of the Aegean, Rhodes, Greece, (liritzis@rhodes.aegean.gr)

Christopher M. Stevenson, Virginia Department of Historic Resources, Richmond, Virginia, USA, (chris.stevenson@dhr.virginia.gov)

CONFERENCE ABSTRACTS ARE NOW AVAILABLE ON THE IAOS WEBSITE:
www.peak.org/obsidian

NOTES FROM THE PRESIDENT

The Society for American Archaeology annual meetings in Vancouver, B.C., were busy with IAOS activities this past March. These included a symposium organized by Rob Tykot with papers reporting obsidian sourcing techniques and research in a wide diversity of locations across several continents. The IAOS Workshop on Sourcing and Dating of Obsidian, organized by Chris Stevenson and Michael Glascock, provided an opportunity for review of current methods and techniques for both obsidian sourcing and hydration analyses. The demonstration of a portable XRF spectrometer was particularly interesting and provided an opportunity for discussion of the pros and cons in using these increasingly popular instruments. Submissions for next year's SAA Meetings in Atlanta will be due in early September. If you are interested in organizing symposia or other events suitable for IAOS sponsorship at these or other professional meetings or workshops, I encourage you to contact me.

Good attendance at the IAOS Annual Meeting allowed for productive discussion of use of the IAOS membership contact list, the status of IAOS officer positions, and proposed changes to the IAOS By-laws. It was agreed that current Secretary-Treasurer Colby Phillips will continue for another two-year term (which requires a change to the By-laws, as discussed below). Two nominations were received for President; additional nominations can be sent to me or the Secretary-Treasurer (to be received by October 1, 2008). Several nominations for the IAOS student poster/paper award were submitted. Most of the nominations were for presentations at the 2008 SAA Meetings. If you know of an excellent student research paper/poster from other conferences this year, contact me so that IAOS can acknowledge their work.

Proposed changes to the IOAS By-laws were prompted during review by the Executive Board this past winter. Several changes are proposed based on this review and subsequent discussion at the Business Meeting. To summarize, we are proposing the elimination of Institutional Member status, change in membership year to calendar year, change in language throughout the By-laws to reflect the use of email as the primary means of communication with the membership, specification of how member contact information will be used, and change in the Secretary-Treasurer office to allow consecutive terms for this position. A copy of the By-laws showing the current text and proposed changes will be posted on the IAOS website at www.peak.org/obsidian Please review the proposed changes and send your comments (to myself or the Secretary-Treasurer) by September 1, 2008. Once member comments are received, a final amended version will be available for a vote by the membership either through email or at the next Business Meeting. We are especially interested in comments from longtime IAOS members on the proposed elimination of the Institutional Member category. While this was a substantive part of the early structure of IAOS, there currently are no active Institutional Members. In reviewing the By-laws, let us know if this category should be eliminated or retained and revitalized.

Ana Steffen
asteffen@unm.edu
asteffen@vallescaldera.gov

IAOS Membership Update

The International Association for Obsidian Studies is in the process of transitioning all IAOS memberships to a Jan. 1 - Dec. 31 calendar year. If you joined or renewed your membership any time last year before Oct. 1 2007, please renew your membership now (you can renew online via PayPal on the IAOS website at http://www.peak.org/~obsidian or simply use the form on the last page of this Bulletin). Renewing your membership will allow the IAOS to continue. If you are unsure about your membership anniversary or last renewal date, please send a message to me at colbyp@u.washington.edu and I will check it for you.

Regards,
Colby Phillips, IAOS Secretary/Treasurer

Field Exploration and Instrumental Neutron Activation Analysis
of the Obsidian Sources in Southern Armenia

John F. Cherry, Brown University
Elissa Z. Faro, Brown University
Leah Minc, Oregon State University

Introduction

The Armenian highlands are an area of intense tectonic activity: within Armenia alone, some 450 volcanic domes have been recorded, and there are as many as 26 reported obsidian outcroppings in the southern Caucasus spread across five Plio-Pleistocene volcanic regions (Blackman et al. 1998: Table 1). Compared to the Mediterranean, Anatolia, and certain other parts of the Near East, field exploration and geochemical characterization of the Armenian obsidian sources has been slow to develop. Since the 1990s, however, much new work has been undertaken — most notably, a comprehensive program of sourcing and provenience studies by Dr. Ruben Badalyan and colleagues, involving the instrumental neutron activation analysis (NAA) of geological hand samples from the majority of the sources and of a further 576 samples derived from 53 archaeological sites throughout the region (Badalyan 2002; cf. Oddone et al. 2000). The most southerly Armenian sources in the Syunik region (at Satanakar, Metz Sevkar, Pokr Sevkar, and Bazenk), however, have not yet been adequately characterized by any of the obsidian research programs of the last two decades (see, e.g., Keller et al. 1994: Table 4, listing analyses of just nine samples). This is unfortunate, since a much earlier study using NAA (Renfrew and Dixon 1977: 145 and Tables 1-2) had suggested that obsidian artifacts of their "Group 3c", all from sites in Iranian Azerbaijan, probably derived from an unlocated Armenian source in, or to the north of, the Lake Urmia region; the Syunik sources (unknown at the time to these authors) are the only ones that come close to matching this description.

The inception in 2005 of the Vorotan Project — a collaborative Armenian-American program of archaeological survey and excavation in the middle reaches of the Vorotan River in Syunik province — has provided an opportunity to conduct more thorough exploration of the Syunik sources, which lie ca. 30 km northwest of the project's main area of focus (Figure 1). Within this latter area, stratified excavation, systematic gridded surface collection of sites, and intensive pedestrian survey conducted by the project have so far yielded a total assemblage of 8,690 pieces of obsidian, whose most likely origin is one or more of the Satanakar, Sevkar, and Bazenk flows. Study has concentrated on documentation and sampling of these flows, as well as secondary obsidian deposits in the Vorotan River, together with morphological, technological, and metrical studies of the assemblages collected by survey and excavation.
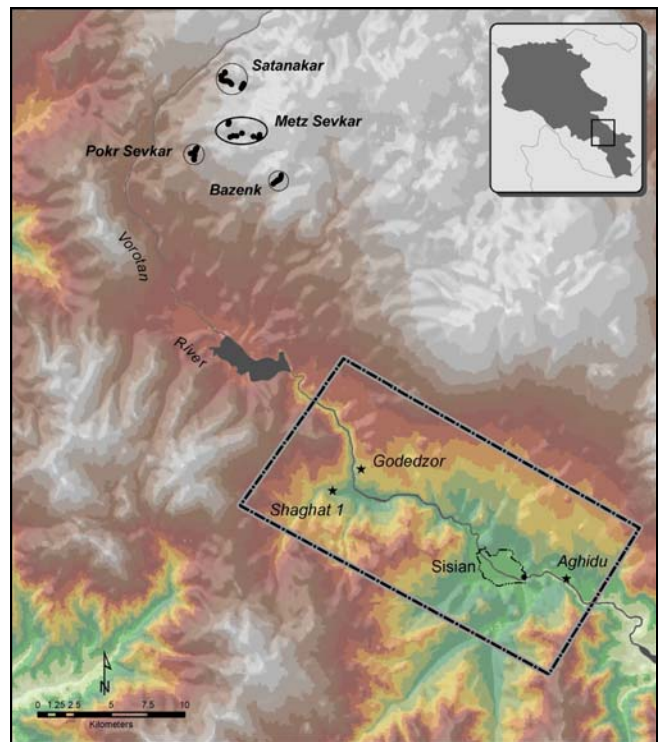

Figure 1. Map showing the location of the southern Armenian Syunik obsidian sources, in relation to the area under study by the Vorotan Project and sites from which obsidian artifacts have been analyzed by INAA. (Map created by Lynn Carlson and Elissa Faro.)

The Syunik Obsidian Flows

The Syunik obsidian flows lie close to the Armenian border with Azerbaijan, in remote and rugged mountainous uplands reaching elevations above 3,200 m. Fieldwork was conducted at all of the geological sources in 2006, with supplementary visits to collect additional samples in 2007. Since these liparite domed volcanoes have already been well described from the geological standpoint (Karapetyan 1972: 73-80), the goals were to locate the various obsidian flows accurately using handheld Trimble GPS/GIS units, to document them photographically, to make systematic collections of geological hand-samples for NAA, and to inspect the evidence for knapping workshops noted, but not described, by earlier visitors (Badalyan et al. 2004: 455-456).

The obsidian occurs within rhyolitic and perlitic flows on the flanks of these volcanoes. It is in general dark gray to jet black, although at the Sevkar sources, uniquely, there are significant occurrences of red-brown mottling; it is translucent when thinly flaked, and for the most part free of perlitization or other crystalline structures that would limit its suitability for knapping. Raw material is available in large blocks between 25 and 75 cm in diameter (sometimes even larger). The abundance of these flows is so great that they can be readily discerned in imagery from space; in one location, on the south flanks of Satanakar, the obsidian outcrops in the form of a spectacular cliff exceeding 50 m in height, with a vast talus slope below it providing a ready source of raw material in convenient form (Figure 2). Indications of knapping activities at the source itself are frequent at Metz and Pokr Sevkar, especially on the slopes of the latter, where macrocores, extremely large core-trimming flakes, portions of blade-cores, blade-flakes, and even large segments of finished blades have been recorded.

Sampling and Analytical Procedures

At least a dozen hand-samples were collected from each source, at regular intervals across as much of the flow as possible, and including examples that reflected macroscopically visible differences in the material (e.g., in terms of color, presence of phenocrysts, etc.). A total of 66 fist-sized geological samples collected in 2006-7 were submitted for trace-element analysis via Instrumental Neutron Activation Analysis (INAA) at the Oregon State University Radiation Center. In addition, 69 pieces of artifactual material from sites within the Vorotan Project study area were included in this analytical program: they come from Chalcolithic, Middle Bronze Age, and Iron Age III ("Yervandid") contexts at the sites of Nerkin Godedzor, Shaghat 1,

Figure 2. View of part of the obsidian cliffs and talus slopes at the Satanakar source, seen from the southwest.

and Aghidu (see Figure 1). Twelve river-rolled cobbles, collected both from the banks of the River Vorotan and during surface survey activities, make up the remainder of the samples.

The obsidian samples were analyzed for a suite of 35 major, minor, and trace elements, through a sequence of two separate irradiations and multiple counts of resultant gamma activity. These two counts provided data on As, Br, La, Lu, Mo, K, Na, Sm, U, Yb, and Ba, Ce, Co, Cr, Cs, Eu, Fe, Hf, Nd, Rb, Sb, Sc, Sr, Ta, Tb, Th, Zn, and Zr, respectively. Elements with short and intermediate half-lives, by contrast, were analyzed using the pneumatic tube irradiation system, which provided data on Al, Ca, Cl, Dy, Mn, K, Na, Ti, and V. Full details of the procedures employed will be presented elsewhere.

Results

The INAA results obtained for the geological samples in this study have been evaluated through a series of bivariate plots of element concentrations, cluster analysis, and principal components analysis. It is apparent that the Bazenk, Satanakar, and Sevkar sources can be clearly discriminated on the basis of their concentrations of the lighter rare earth elements (especially La and Ce) and Th. The separation of these sources is illustrated in Figure 3, which uses the elements La and Th; ellipses around the subgroups are plotted at the 95% confidence level. Samples from Pokr Sevkar and from widely separate areas of the Metz Sevkar source display generally overlapping elemental compositions, and it is possible to treat these flows together as the "Greater Sevkar" complex, which itself constitutes a fairly tight group. Satanakar has provided trace elemental evidence of two quite clearly distinguishable flows, which also map onto the volcano in a spatially coherent manner.

The assignment of obsidian artifacts to their most likely geological source shows a strong preference for the Greater Sevkar flows (Figure 4). This is an unsurprising result, given that they are geographically very extensive, at lower altitude, and more readily accessible than the other two sources. Artifactual samples from late
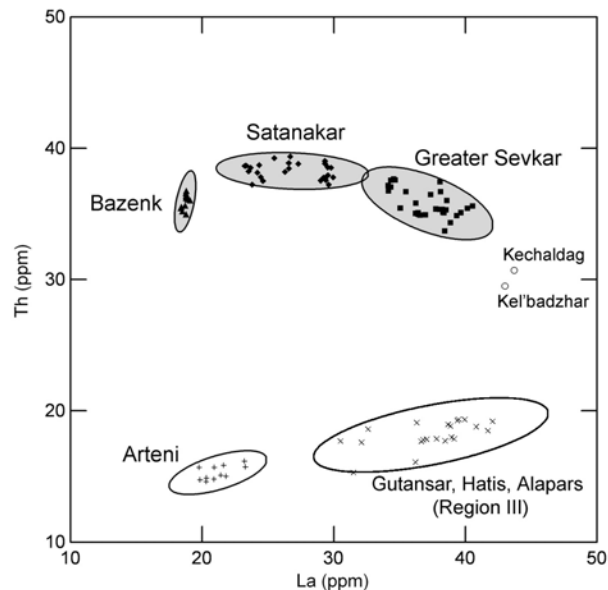

Figure 3. Bivariate plot of La and Th showing the NAA data obtained from geological hand-samples collected at the Bazenk, Satanakar, Metz Sevkar, and Pokr Sevkar obsidian sources. Ellipses around the subgroups are plotted at the 95% confidence level.

Chalcolithic Godedzor (made available to us courtesy of Dr. Pavel Avetisyan) are dominantly of Sevkar obsidian, but with minor use of the Satanakar and Bazenk sources too, and no evidence for exploitation of any other Armenian obsidian source. All the samples from Shaghat 1 (mainly Middle Bronze Age, but a few from mid- to late-1st millennium B.C. contexts) are attributable to the Sevkar flows, with the exception of a single artifact that appears closest in composition to published data on samples from volcanic groups in the northern part of Region III in central Armenia (Keller et al. 1994: 71, figs. 1, 3; see also Blackman et al. 1998; Oddone et al. 2000). Lastly, obsidians from the Iron Age III (mid-first millennium B.C.) citadel at Aghidu are once again dominantly from Sevkar, with a single example from Bazenk and another probably from the Kecheldag/Kel'badzhar source, which lies just across the border in Azerbaijan (and thus could not be included in the present program of fieldwork).
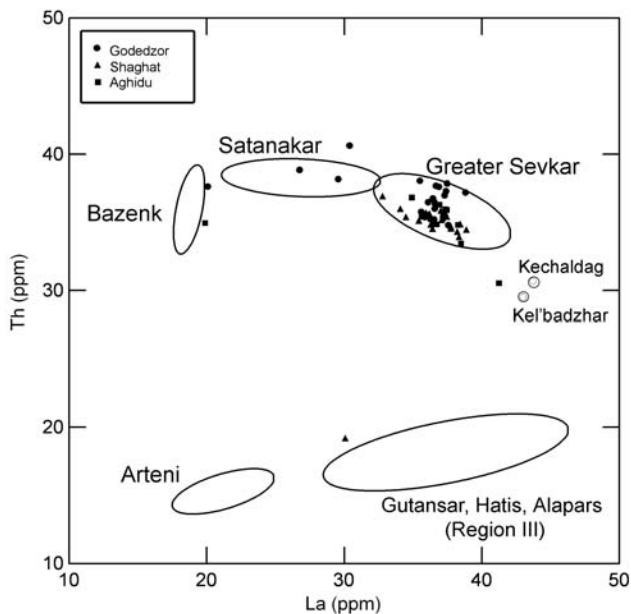
Figure 4. Bivariate plot of La and Th showing the NAA data obtained from artifacts collected at the sites of Godedzor, Shaghat 1, and Aghidu, plotted against the 95% confidence-level ellipses established for the Bazenk, Satanakar, and Greater Sevkar sources.

Conclusions

It comes as little surprise that the occupants of sites only a few dozen kilometers from the high-quality Syunik obsidian sources should have relied on them almost exclusively. On the other hand, since they occur at such high altitude, these sources would have been inaccessible for more than half the year, and it is likely that the rolled obsidian cobbles available as a secondary deposit along the River Vorotan constituted a raw material resource equal in importance to the flows *in situ*. Now that the Syunik sources have been much more thoroughly characterized than hitherto, the logical next step is a comprehensive program of analysis of obsidian artifacts from Azerbaijan, northwestern Iran, Nakichevan, and southeastern Anatolia, in order to establish the regional scale of the exploitation of these sources (and whether they have any connection to the "3c source" identified long ago by Renfrew and colleagues). We also intend to explore the metrical aspects of the archaeological assemblage in greater detail, as well as seeking an explanation for a dramatic decline in the abundance of obsidian artifacts after the Middle Bronze Age.

References

Badalyan, R.
2002 *Obsidian Kavkaza: Istochniki I Rasprostranenie Siria v Epokhu Neolita-Rannevo Zheleza (po Resultatam Analizov Neutronnoy Aktivatzii)*. Unpublished PhD dissertation, Institute of Archaeology and Ethnography, Yerevan.

Badalyan, R., C. Chataigner, and P.L. Kohl
2004 Trans-Caucasian obsidian: the exploitation of the sources and their distribution. In A. Sagona (ed.), *A View from the Highlands: Archaeological Studies in Honour of Charles Burney*, 437-465. Leuven: Peeters.

Blackman, J., R. Badaljan, Z. Kikodze, and P.Kohl
1998 Chemical characterization of Caucasian obsidian geological sources. In M.-C. Cauvin, A. Gourgaud, B. Gratuze, N. Arnaud, G. Poupeau, J.-L. Poidevin, and C. Chataigner (eds.), *L'obsidienne au Proche et Moyen Orient: du volcan à l'outil*. BAR International Series 738: 205-31. Oxford: Archaeopress.

Karapetyan S.G.
1972 *Osobennosti stroenia I sostava novejshikh liparitovykh vulknov Armianskoj SSR*. Yerevan.

Keller, J., R. Djerbashian, S.G. Karapetian, E. Pernicka, and V. Nasedkin
1994 Armenian and Caucasian obsidian occurrences as sources for the Neolithic trade: volcanological setting and chemical characteristics. In S. Demirci, A.M. Özer, and G.D. Summers (eds.), *Archaeometry 94: The Proceedings of the 29th International Symposium on Archaeometry, Ankara, 9-14 May 1994*, 543-551. Ankara: TÜBITAK.

Oddone, M., G. Bigazzi, Y. Keheyan, and S. Meloni
2000 Characterisation of Armenian obsidians: implications for raw material supply for prehistoric artifacts.*Journal of Radioanalytical and Nuclear Chemistry* 243: 673-82.

Renfrew, C., and J. Dixon
1977 Obsidian in western Asia: a review. In G. de G. Sieveking, I.H. Longworth, and K.E. Wilson (eds.), *Problems in Economic and Social Archaeology*, 137-150. Boulder: Westview Press.

A Geochemical Investigation of Obsidian Artifacts from Sites in Northwestern Iran

Soheila Ghorabi[1], Michael D. Glascock[2], Farhang Khademi[1],
Abdulhamid Rezaie[1] and Mohammad Feizkhah[3]
[1]Department of Archaeology, Tarbiat Modares University, Tehran, Iran
[2]Research Reactor Center, University of Missouri, Columbia, MO, USA
[3]Department of Archaeology, Azad University of Miyaneh, East Azerbaijan, Iran

Introduction

The discovery of obsidian on archaeological sites in eastern Anatolia and the surrounding regions shows that obsidian utilization took place over a long period of time from at least the early Neolithic through Bronze Age. Renfrew et al. (1966; 1968) demonstrated that the chemical compositions of obsidian artifacts could be used to reconstruct obsidian exchange networks involving the Anatolian sources. As a result, archaeologists have subdivided the ancient Near East into regions according to the particular source(s) utilized. A few of the Near Eastern obsidian sources were associated with long-distance exchange networks, but many obsidians did not travel far from their origin.

Background

Studies of obsidian in Iran have not progressed as rapidly as in other regions resulting in an imperfect model for regional source utilization. Using XRF and NAA to characterize obsidian artifacts from the archaeological sites at Salmas and Kaleybar in NW Iran (see Figure 1), new information suggests the possible existence of obsidian sources in NW Iran (candidate locations for obsidian sources are Mt. Sabalan and Mt. Sahand). Models of obsidian exchange in Iran should therefore consider these "new" sources along with currently known obsidian sources in the Lake Van region of eastern Turkey and in the countries of Armenia and Azerbaijan (Blackman et al. 1998; Chataigner et al. 1998; Keller et al. 1996). The obsidian sources already known to this region are shown in Figure 1.

Archaeological Sites of Salmas and Kaleybar

The Salmas Plain (1560 m above sea level) is located in the West Azerbaijan province of Iran about 20 km west of Lake Urmia and 35 km east of the border with Turkey. The Salmas Plain was occupied continuously from the Neolithic to the Bronze Age. Evidence indicates that the earliest
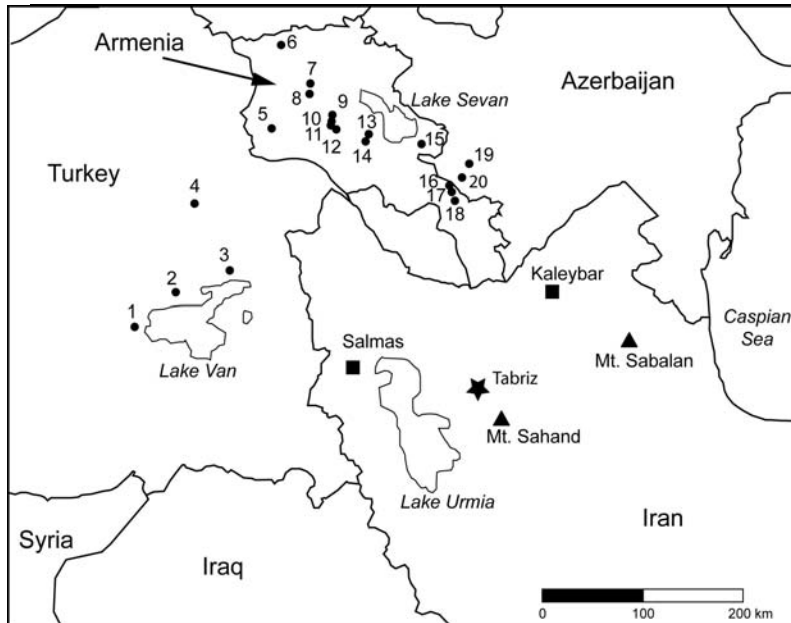

Figure 1. Map showing the locations of archaeological sites of Salmas and Kaleybar, the known obsidian sources in Eastern Turkey and the Caucasus region, possible obsidian sources in Iran at Mt. Salaban and Mt. Sahand. Locations of known obsidian sources from Blackman et al. (1998) and Keller et al. (1996) are labeled: 1=Nemrut (four compositional types), 2=Suphan, 3=Maydan, 4= Sarikamis, 5=Arteni (three compositional types), 6=Ashotsk (two compositional types), 7=Hankavan, 8=Kamakar, 9= Alaphars, 10=Fontan, 11=Gutansar, 12= Hatis, 13=Spitaksar, 14=Geghasar, 15= Choraphor, 16=Satanakar (three compositional types), 17=Sevkar, 18= Bazenk, 19=Kelbedzhar, and 20=Ketchal.

inhabitants of Salmas were primarily agricultural and they used tools made of bone, ground stone, and obsidian as early as the the 6th millenium. Approximately 200 obsidian artifacts with colors primarily black and grey, have been discovered at sites in the Salmas Plain (Kargar 1996) indicating that the occupants had access to obsidian sources. The nearest sources to Salmas are located in the Lake Van region with distances ranging from 150-200 km. A total of seven obsidian artifacts from the Salmas region were made available for compositional analysis by Mr. Kargar.

The Kaleybar sites are located in the Kaleybar township of the East Azerbaijan province a distance of about 110 km northeast of the city of Tabriz and 40 km from the Aras River which serves as the border between Iran and the country of Azerbaijan. Numerous settlements from the Chalcolithic and Urartu periods are found throughout Kaleybar. Obsidian artifacts are found in greater abundance in the Kaleybar regions indicating that access to obsidian sources was probably greater (Feizkhah 2007). The nearest known sources are located in Armenia and Azerbaijan, but it is possible that cobbles of obsidian were extracted from the Aras River or from yet to be discovered sources in Iran. Mr. Feizkhah made a total of 38 obsidian artifacts from Kaleybar available for geochemical analysis.

Analytical Methodology

A combination of the two most reliable analytical techniques for obsidian characterization – X-ray fluoresence (XRF) and neutron activation analysis (NAA) – were employed in this investigation using the facilities available in the Archaeometry Laboratory of the University of Missouri Research Reactor Center. The advantages of XRF and NAA are well known. In short, XRF is non-destructive, more rapid, and less expensive; however, XRF measures fewer elements, has less precision, and is less accurate than NAA. By employing both methods to our study, we were able to maximize the advantages of both techniques. The entire collection of 45 of the obsidian artifacts were analyzed by XRF in order to sort the artifacts into specific geochemical types. Afterwards, a sub-sample consisting of 22 artifacts, selected to include all possible varieties, were characterized by NAA to obtain high

precision data and allow direct comparison to obsidian source data reported earlier by Blackman et al. (1998) and Keller et al. (1996).
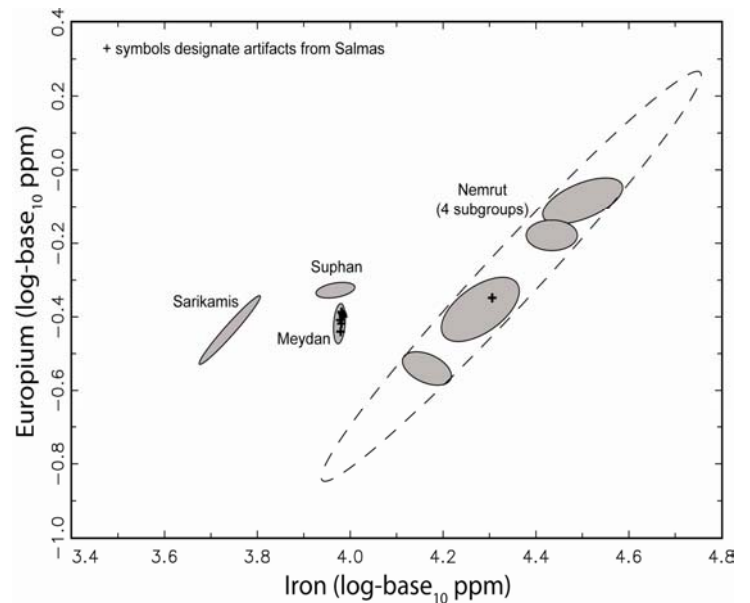

Figure 2a. Plot of Iron versus Europium showing NAA data for obsidian artifacts from Salmas projected against 95% confidence ellipses for obsidian sources in the Lake Van region. The Nemrut source has four subgroups.
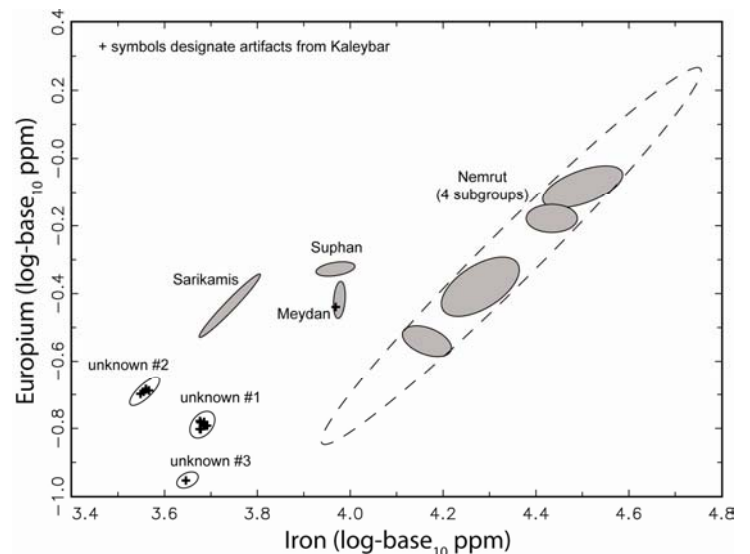

Figure 2b. Plot of Iron versus Europium showing NAA data for obsidian artifacts from Kaleybar projected against 95% confidence ellipses for obsidian sources in the Lake Van region. The Nemrut source has four subgroups. The unknown sources do not match any of the published data for obsidian sources in Turkey or the Transcaucasus region.

Table 1. Summary of sourcing results for artifacts from the sites of Salmas and Kaleybar.

Source name	Salmas	Kaleybar
Meydan	6	1
Nemrut	1	0
Unknown Group #1	0	31
Unknown Group #2	0	5
Unknown Group #3	0	1
Total	7	38

Table 2. Concentrations of elements measured by NAA in groups of obsidian unknowns from Kaleybar.

Element	Unknown Group #1 (n = 8)			Unknown Group #2 (n=5)			Unknown Group #3 (n=1)
Ba (ppm)	64	±	13	46	±	5	62
La (ppm)	33.5	±	0.5	17.0	±	0.5	27.3
Lu (ppm)	0.396	±	0.012	0.622	±	0.013	0.456
Nd (ppm)	12.1	±	1.1	12.2	±	0.9	9.8
Sm (ppm)	2.39	±	0.06	3.93	±	0.12	2.16
U (ppm)	10.0	±	0.3	15.1	±	0.3	11.7
Yb (ppm)	1.45	±	0.02	2.39	±	0.05	1.47
Ce (ppm)	56.2	±	0.8	36.0	±	1.4	45.9
Co (ppm)	0.130	±	0.016	0.105	±	0.047	0.093
Cs (ppm)	4.48	±	0.08	7.48	±	0.19	5.16
Eu (ppm)	0.162	±	0.003	0.204	±	0.003	0.111
Fe (ppm)	4807	±	66	3612	±	57	4425
Hf (ppm)	3.68	±	0.05	3.11	±	0.06	3.73
Rb (ppm)	173	±	3	200	±	3	190
Sb (ppm)	0.212	±	0.006	0.631	±	0.024	0.237
Sc (ppm)	1.74	±	0.04	3.08	±	0.06	1.97
Sr (ppm)	< 15			< 15			< 15
Ta (ppm)	2.17	±	0.04	4.49	±	0.11	2.29
Tb (ppm)	0.188	±	0.005	0.509	±	0.019	0.152
Th (ppm)	32	±	1	27	±	1	35
Zn (ppm)	37	±	3	34	±	1	39
Zr (ppm)	165	±	5	180	±	8	163
Al (%)	6.85	±	0.24	7.07	±	0.06	6.76
Cl (ppm)	319	±	36	215	±	17	335
Dy (ppm)	1.35	±	0.34	3.48	±	0.30	1.49
K (%)	3.89	±	0.07	3.70	±	0.22	3.89
Mn (ppm)	463	±	6	669	±	11	520
Na (%)	3.06	±	0.03	3.17	±	0.03	3.17

Results

Five different geochemical types were identified among the 45 artifacts as shown in Figure 2a, Figure 2b and Table I. As shown in Figure 2a, the obsidian artifacts from Salmas were traced to two of the well-known Lake Van sources – one artifact came from the Nemrut source and six came from the Meydan source. There is little surprise here since the Lake Van sources are located closest to Salmas. However, as shown in Figure 2b, the artifacts from Kaleybar proved to be more interesting. Four different geochemical types were identified; however, only one of the artifacts to could to traced to a known source. The single sample was traced to the Meydan obsidian source. The remaining 37 artifacts subdivide into three geochemical types: unknown #1 which has 31 artifacts, unknown #2 which has five artifacts, and unknown #3 which has one artifact. Comparisons of the NAA data from MURR with the data from Blackman et al. (1998) were unsuccessful in linking the artifacts to any of the known sources in Turkey, Armenia or Azerbaijan. Table II lists the calculated means and standard deviations for the three new obsidian source types identified during this investigation.

Discussion and Future Research

We conclude that the three newly established geochemical types are probably from sources in Iran (possibly Mt. Sahand or Mt. Sabalan) or from sources in the Transcaucasus that have yet to be reported. The Kaleybar site is relatively close to Mt. Sabalan and our data strongly suggest this area ought to be searched to locate possible obsidian deposits. The distance to Mt. Sahand is much greater but the area surrounding this volcanic peak should also be inspected to determine if any of the unknown artifacts at Kaleybar could have come from a source in that area.

Acknowledgements

References

Blackman, M.J., R. Badalian, Z. Kikodze, Ph. Kohl
1998 Chemical characterization of Caucasian obsidian geological sources. In Cauvin, M.C.; Gourgaud, A.; Gratuze, B.; Arnaud, N.; Poupeau, G.; Poidevin, J.L.; Chataigner, C. (eds.), *L'obsidienne au Proche et Moyen Orient*, BAR Intl Series 738, pp. 205-231.

Chataigner, C., J. L. Poidevin, N. O. Arnaud
1998 Turkish occurences of obsidian and use by prehistoric peoples in the Near East from 14,000 to 6000 B.P. *J. Volcano. Geotherm. Res.*, 85: 517-537.

Feizkhah, M.
2007 Archaeological Survey and Exploration at the Khodafarin and GizGalasi dams. Report to the ICHTO Iranian Center for Archaeological Research.

Kargar, B.
1996 Sondages and Survey of Aharnjan Tepe and Qara Tepe in the Salmas Plain. M.A. thesis, Dept. of Archaeology, Tehran University.

Keller, J., R. Djerbasian, S. G. Karapetian, E. Pernicka, V. Nasedkin
1994 Armenian and Caucasian obsidian occurrences as sources for the Neolithic trade: volcanological setting and chemical charateristics. In Demirci, S.; Ozer, A.M.; Summers, G.D. (eds), *Archaeometry 94, The Proceedings of the 29th Symposium on Archaeometry, Ankara 9-14 May 1994*, Tubitak, Ankara, pp. 69-86.

Renfrew, C., J. E. Dixon, J. R. Cann
1966 Obsidian and early cultural contact in the Near East. *Proc. Prehist. Soc.*, 32: 30-72.
1968 Further analysis of Near Eastern obsidians. *Proc. Prehist. Soc.,* 34: 319-331.

A New Look at the Geochemistry of Obsidian from East Africa

Magen E. Coleman[1], Jeffrey R. Ferguson[2], Michael D. Glascock[2], J. David Robertson[1,2], and
Stanley H. Ambrose[3]
[1]University of Missouri, Department of Chemistry, [2]University of Missouri, Research Reactor
Center, and [3]University of Illinois, Department of Anthropology

African Obsidian and the Origins of Modern Human Behavior

Databases of obsidian sources have been created for many parts of the world, but as of yet no comprehensive database exists for East Africa. Though some studies have been done on obsidian from this region, most notably Merrick and Brown (1984a,b & 1994), for the most part, they have not been comprehensive (Michels et. al. 1983; Negash et al. 2006a, 2006b, 2007). In addition, these data have not been collected in a manner conducive to the incorporation of new data collected using different analytical methods, and geographical coordinates for sources remain unpublished. However, these studies have shown the great potential for creating a comprehensive database for this region.

The work presented here is part of a continuing effort to create such a database by analyzing source samples from known sources to chemically characterize the geochemistry of the region, gathering the data from previous studies into one database to make it more easily accessible, and analyzing artifacts from this region to test the database and its ability to source artifacts accurately. The database will then be used to study obsidian source exploitation patters to evaluate models of mobility, exchange, and interaction in ancient East Africa. This work focuses first on the analysis of the sources located in the Central Rift Valley in Kenya, a region rich in high-quality obsidian sources that were often used by ancient peoples.

One application of such a database is to examine the transition of humans to fully modern behavior (Ambrose 2001, 2002; Ambrose in press; Barut 1994). During the Middle Stone Age (MSA)/Late Stone Age (LSA) transition, we see a shift toward the development of socio-political organizations similar to ethnographically observed hunter-gatherers. This shift in organization is accompanied by changes in the patterns of raw material procurement. Typically, procurement of raw materials outside of the zone of direct procurement follows a distance-decay pattern, i.e. as the distance between a site and a source increases the relative abundance of that source decreases. However, as the interaction between socio-political groups increases, the slope of the typical distance-decay curve becomes shallower, as more artifacts from non-local materials are found at greater distances. Variation in mobility and home range size should also influence the slope of a curve and the size of the direct procurement zone. Hunter-gatherer home ranges are larger and social networks are more extensive and intensive in less productive, arid environments. Steeper slopes and smaller direct procurement zones should be found when higher rainfall supports more stable and productive environments (Ambrose 2002).
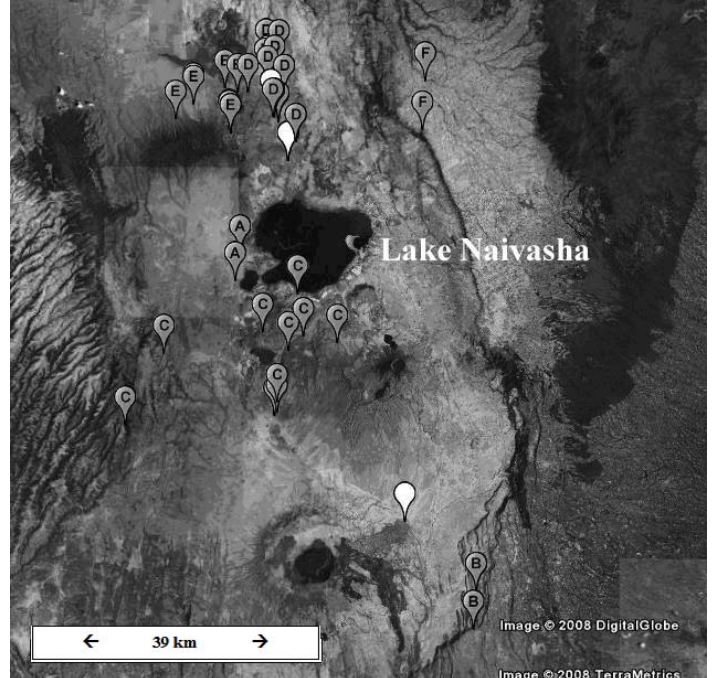

Figure 1. Location of obsidian sources in the central Rift Valley of Kenya analyzed in this study. Six chemical groups are plotted geographically. The white symbols represent chemically isolated samples.
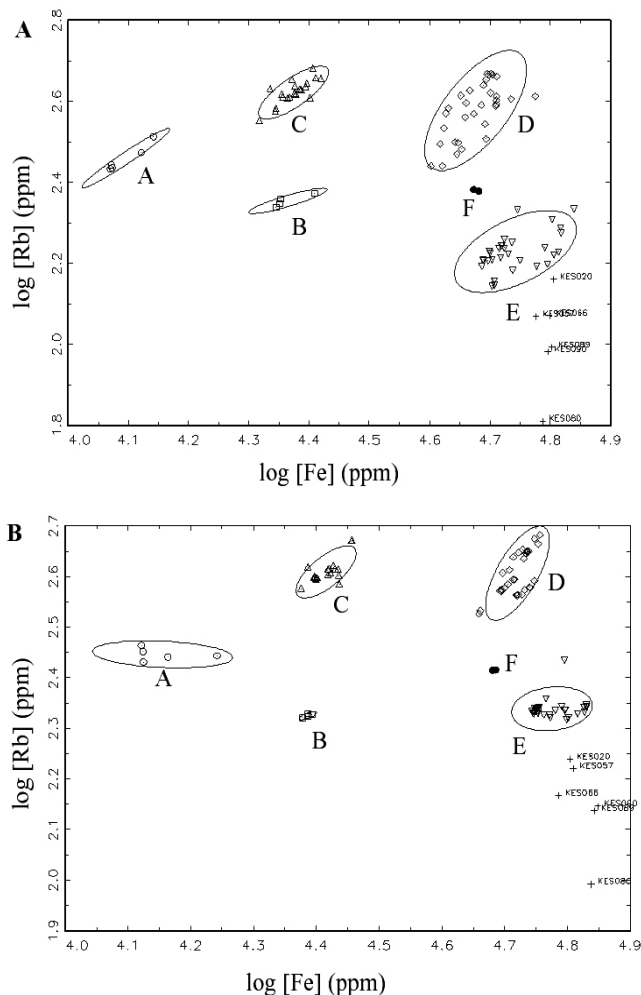
Figure 2. A comparison between the XRF and NAA groupings. Figure 2A shows the results from XRF while Figure 2B shows the results from NAA. Both plots show the same groupings, though the groups formed with the NAA data are better resolved than those from the XRF data.

Methodology

The Central Rift Valley in Kenya was chosen as a good starting place, as there have been some studies done on obsidian from this general region, but there are many sources that are not sufficiently characterized (Ambrose in press). One hundred source samples were acquired by Dr. Stanley Ambrose of the University of Illinois for chemical analysis from 2001 to 2006 (Figure 1). The concentrations of trace elements are used to characterize the sources. The best elements are those incompatible with the solid phase due to

large ion size or high ionic charges. One of the incompatible groups consists of the large-ion lithophile elements (LILE which include K, Rb, Cs, Sr, and Ba), the light rare earth elements (LREEs, La to Sm), and Th and U. Another of the incompatible groups consists of the high field-strength elements (HFSE which include Y, Zr, Hf, Nb, and Ta) and the heavy rare earth elements (HREEs, Eu to Lu). Many of these elements can be measured with excellent precision and accuracy using either XRF or NAA.

X-ray fluorescence (XRF) is a nondestructive technique that uses secondary x-rays to characterize the chemical composition of a sample. In XRF analysis, an x-ray of sufficient energy strikes the sample and is absorbed by the atoms causing the ejection of inner electrons. This puts the atom in an excited state and electrons from the outer shells are quickly transferred to fill the vacancies, giving off an x-ray in the process. These secondary x-rays are characteristic of the element that was struck by the primary x-ray and their energy is equal to the difference between the shell initially occupied by the electron and the shell it occupies after filling the vacancy. XRF is completely nondestructive, an important feature for the analysis of artifacts. The concentrations of eleven elements (K, Ti, Mn, Fe, Zn, Ga, Rb, Sr, Y, Zr, and Nb) in ppm are usually determined (Glascock 1998).

In neutron activation analysis (NAA), the sample is irradiated with neutrons, inducing radioactivity in the sample. These induced isotopes emit gamma rays as they decay to stable isotopes. The intensity of the gamma-ray emission is proportional to the original concentration of the element in the sample. NAA, due to the induced radioactivity, is a destructive technique. Typically, samples of about 100 milligrams are removed and used for analysis. Data acquired from NAA is typically more precise and more accurate than that obtained from XRF analysis. The relative concentrations of twenty-eight elements (Al, Ba, Ce, Co, Cs, Cl, Dy, Eu, Fe, Hf, K, La, Lu, Mn, Nd, Na, Rb, Sb, Sc, Sr, Sm, Ta, Tb, Th, U, Yb, Zn, and Zr) are determined by NAA (Glascock 1998). Neutron activation analysis was performed at the University of Missouri Research Reactor under the guidance of Dr. Michael Glascock.

For obsidian, simple bivariate plots can be used to identify source groups and compare compositional groups to geographic locations. The groups can then be validated statistically using Euclidean distances. Principal component analysis will also be used to

confirm that the best results are being acquired from the groups and the elements used to distinguish those groups, once there are enough samples to make the results statistically valid (Glascock 1998).
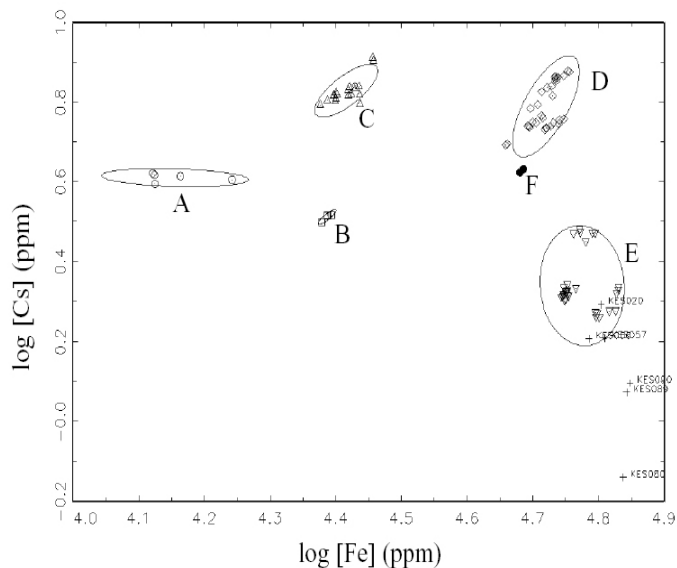

Figure 3. Plot of cesium versus iron. As can be seen most clearly in the group to the far right, some subgroups can be seen in some bivariate plots. However, more samples need to be analyzed to confirm the presence of these subgroups. In addition, there is a clear split in the iron concentration with the three groups on the left corresponding to the samples found south of the lake while the other groups correspond to the samples north of the lake.

Preliminary Results and Discussion

Thus far, the results are promising. The 100 source samples fall into at least six major chemically-distinct groups, with strong evidence for a few of those groups to be separated into subgroups. Plots of the rare earth elements and a few of the large-ion elements versus iron showed the greatest separation between groups. Looking at the XRF results, a plot of the log of the concentration of rubidium in parts per million (ppm) versus that of iron showed the best separation of the major groups (Figure 2). However, better resolution is needed in order to see subgroups. Using the NAA data, plots of cesium and the rare earth elements versus iron

clearly show separation occurring within a few of the major groups, separating samples into subgroups.

In comparing these chemical source groups to their geographic locations, the samples fell into the same groupings with only a small amount of overlap between some possible subsources (Figure 1). Also, there appears to be a correlation between the concentration of iron and the location. Samples from the southern-most groups tend to have a lower concentration of iron (<3.0%) while northern samples tend to have a higher iron concentration (>4.5%) (Figures 1 and 3). In both cases, the iron concentration is relatively high, indicating that this region produced obsidian with peralkaline tendencies.

Future Work

Though the results of this study seem promising, a lot more work in this area must be done in order to distinctly characterize the geochemistry of this region of Africa as well as other regions. First, more samples will be collected from many of the sources examined in this study to confirm groupings, assess intra-source variation, and to improve statistics. Second, samples from outside the central Rift region will be collected to compare to these few original groups to gain a better understanding of the geochemistry of this area. Third, the results from previous studies done in this region will be compared with the results from this study to create a comprehensive database for these sources. Finally, artifacts will be obtained to test the completeness of the database and to begin applying the database to specific archaeological questions. Artifacts from several archaeological sites in Kenya do not match known sources (Merrick and Brown 1984; Merrick et al., 1994). An expanded source database would permit more comprehensive determination of site-to-source distances, and provide a firmer foundation for evaluating mobility, exchange and interaction patterns during the final stages of the evolution of modern human behavior. This database will be equally useful for understanding exchange and interaction patterns in later prehistory, particularly during the Neolithic era.

References

Ambrose, S.H.

2001 Middle and Later Stone Age settlement patterns in the Central Rift Valley, Kenya: comparisons and contrasts, *Settlement Dynamics of the Middle Paleolithic and Middle Stone Age*, N. J. Conrad, Ed., Kerns Verlag: Tubingen, pp. 21-43.

2002 Small things remembered: Origins of early microlithic industries in Sub-saharan Africa. In *Thinking Small: Global Perspectives on Microlithization*. Elston, R. G. and S. L. Kuhn (eds). Archaeological Papers of the American Anthropological Association. Washington, pp. 9-29.

In press Obsidian Dating and Source Exploitation Studies in Africa: Implications for the Evolution of Human Behavior. In *The Dating and Provenance of Obsidian and Ancient Manufactured Glasses,* Stevenson, C., W. R. Ambrose and I. Liritzis, (eds.) University of New Mexico Press, Albuquerque.

Barut, S.

1994 Middle and Later Stone Age lithic technology and land use in East African savannas. *The African Archaeological Review*, 12: 43-72.

Glascock, M., G.E. Braswell, & R.H. Cobean

1998 A Systematic Approach to Obsidian Source Characterization. In *Archaeological Obsidian Studies: Method and Theory*. Shackley, M.S. (ed.), Plenum Press: New York, pp. 15-65.

Merrick, H.V. & F.H. Brown

1984a Rapid Chemical Characterization of Obsidian Artifacts by Electron Microprobe Analysis. *Archaeometry*, 26(2), 230-236.

1984b Obsidian sources and patterns of source utilization in Kenya and northern Tanzania: some initial findings. *The African Archaeological Review*, 2: 129-152.

Merrick, H.V., F.H. Brown, & W.P. Nash

1994 Use and Movement of Obsidian in the Early and Middle Stone Ages of Kenya and Northern Tanzania. In *Society, Culture, and Technology in Africa*; Childs, S. T., (ed.), Vol. 11, p 29-44.

Michels, J.W., I.S.T. Tsong, and C.M. Nelson

1983 Obsidian Dating and East African Archaeology. *Science*, 219: 361-366.

Negash, A., M. Alene, and M.S. Shackley

2006a Geochemical Provenance of Obsidian from the MSA Site of Porc Epic, Ethiopia. *Archaeometry* 48:1-12

2006b Source provenance of obsidian artifacts from the Early Stone Age (ESA) site of Melka Konture, Ethiopia. *Journal of Archaeological Science*, 33:1647-1650

Negash, A., M. Alene, F.H. Brown, B.P. Nash & M.S. Shackley

2007 Geochemical sources for the terminal Pelistocene.eary Holocene obsidian artifacts of the site of Beseka, central Ethiopia. *Journal of Archaeological Science*, 34(8): 1205-1210.

Regional Scaling for Obsidian Hydration Temperature Correction

Alexander K. Rogers, Maturango Museum

Abstract

Hydration of obsidian is a temperature-dependent process, and correcting for temperature history is necessary for chronological use of obsidian hydration data. This paper describes a technique for estimating temperature history for an archaeological site, in which all the nearby sites in the same weather patterns are analyzed and a best scaling algorithm determined. The method uses data from publicly-available meteorological records. Two case studies are presented to illustrate the technique.

Introduction

It is well known that obsidian hydration is a temperature dependent process, and that temperature at an archaeological site varies both diurnally and annually (e.g. Friedman and Long 1976; Stevenson et al.1989, 1998, 2000, 2004; Rogers 2007). Thus, the effects of temperature history, manifested as effective hydration temperature (EHT) must be taken into account in any use of obsidian hydration data for chronological analyses. Computing a correction for temperature requires estimates of three temperature parameters: annual average temperature, annual temperature variation, and mean diurnal variation (Rogers 2007a). Furthermore, the temperature parameters must be representative of long-term conditions at the site; meteorological practice describes such data as norms, and typically demands a 30-year history (Cole 1970). Since most archaeological sites are not collocated with a modern weather station, estimating these parameters can present a problem.

This paper describes a technique of regional temperature scaling or estimation, in which all the nearby sites are analyzed and a best scaling algorithm determined. This has the advantage that it makes use of all the data available, and averages the effects of microclimates to some degree, with the caveat that the sites chosen must be in the same general weather patterns. The method is based on publicly-available meteorological records, from the web sites of the Regional Climate Centers. Two case studies to illustrate the technique are presented.

Alternative techniques involve temperature sensors at the archaeological site, or scaling from the nearest site, both of which have drawbacks. Temperature sensors placed at the site will yield short-term estimates, but these may not be representative of long-term conditions. Alternatively, estimates have been based on the nearest site with long-term temperature data, scaled for altitude by the mean adiabatic lapse rate (e.g. Gilreath and Hildebrandt 1997), but this procedure runs the risk that local microclimatic effects may affect the extrapolation. The method described herein avoids both these problems.
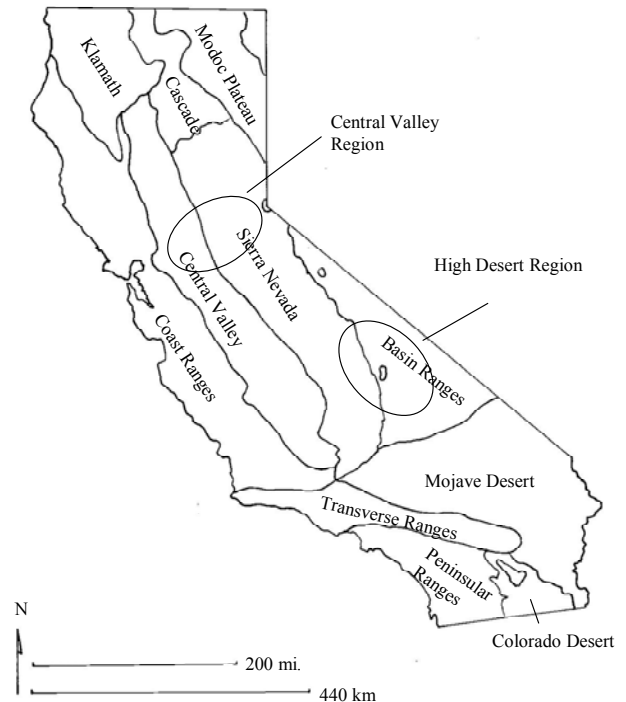

Figure 1. Map of California, showing regions used for temperature scaling case studies.

Analytical Technique

Computation of effective hydration temperature (EHT) is based on the equation (Rogers 2007a)

$$EHT = T_a(1 - 3.8 \times 10^{-5}\, Y) + .0096Y^{0.95} \quad (1a)$$

$$Y = V_a^2 + V_d^2. \quad (1b)$$

This requires three temperature parameters for the site: annual average temperature (T_a); annual temperature variation (V_a), defined as the difference between the July average temperature and the January average temperature; and mean diurnal variation (V_d), defined as the average of the daily temperature ranges for July and January.

The two variation parameters, V_a and V_d, represent the conditions to which an artifact was exposed, and thus are subject to corrections for depth (Carslaw and Jaeger, 1959: Rogers 2008; Stevenson et al. 1989) and for rock shelters (Everett-Curran et al. 1991; Rogers 2007a). The present analysis considers effects at the surface, so these corrections do not apply.

The validity of EHT as computed from equation 1 and this temperature model has been verified by comparison with EHT computed from actual hourly temperature data from the Amargosa Desert Research Site (Johnson et al. 2002, amplified by data through 2005); the standard deviation of the error between the two was <0.89°C (Rogers 2008).

For the analysis here, temperature data for the desired sites are downloaded from the appropriate Regional Climate Center. The temperature parameters are then computed from the equations

$$T_a = (\text{annual max temp.} + \text{annual min temp.})/2 \quad (2)$$

$$V_a = (\text{Jul max} + \text{Jul min})/2 - (\text{Jan max} + \text{Jan min})/2 \quad (3)$$

$$V_d = [(\text{Jul max} - \text{Jul min}) + (\text{Jan max} - \text{Jan min})]/2 \quad (4)$$

and converted to °C. These parameters are then analyzed to determine the most appropriate and robust scaling method.

Two cases are described as examples; the locations are shown in Figure 1. The first is based on sites in the high desert of eastern California, and is typical of desert mountain regions with significant altitude relief. It spans a region roughly 200 km east-west by 300 km north-south, east of the Sierra Nevada, centered around a latitude of approximately 36°48′ N. The second is the central area of the Central Valley of California and its eastern foothills and Sierra slope, with Sacramento at its western edge, extending east to Nevada City. It extends roughly 200 km north-south and 100 km east-west, centered on a latitude of 38°30′ N. This region is typical of extended valleys and foothills, in which the climate is dominated by a temperature inversion layer. It will be seen that different scaling techniques are required for these two cases.

All the temperatures used in this study are air

Station	Alt, ft	Ave Max, deg F	Ave Min, deg F	Annual Ave, deg F	Jul Max, deg F	Jul Min, deg F	Jan Max, deg F	Jan Min, deg F
Baker	940	86.2	54.0	70.1	110.0	74.9	63.4	34.9
Trona	1700	80.1	54.0	67.1	102.0	73.6	59.0	36.1
Daggett Apt	1930	81.7	54.4	68.1	104.2	73.4	61.3	37.5
Cantil	1960	80.1	47.5	63.8	104.3	69.2	58.9	28.9
Barstow	2140	79.8	47.1	63.5	101.9	66.0	60.2	31.7
China Lake Armitage Fld	2240	80.5	47.0	63.8	100.6	67.2	59.9	32.3
Inyokern	2440	80.9	47.4	64.2	102.4	65.9	60.5	31.1
Mojave	2740	75.9	49.5	62.7	96.6	68.3	57.7	33.6
Haiwee	3282	73.6	45.1	59.4	95.7	63.8	52.7	29.1
Randsburg	3570	74.7	50.5	62.6	97.4	67.6	54.3	36.4
Wildrose	4100	72.3	45.2	58.8	95.0	63.4	51.6	30.1
Mtn Pass	4740	70.7	45.0	57.9	92.3	65.3	51.1	29.4
WhiteMtn	11811	46.7	20.4	33.6	66.6	37.0	33.5	8.6

Table 1. Temperature data for high desert sites.

temperatures with 30 years of history, measured two meters above the ground in an enclosure which shelters the sensor from direct sunlight, normal meteorological practice.

High Desert

This case demonstrates a situation in which two of the three temperature parameters show strong scaling with site altitude. The analysis is based on monthly temperature data from the Western Regional Climate Center (WRCC), using the data base from 1971 – 2000. Table 1 summarizes the sites used in the temperature scaling analysis. All are from desert or desert mountain environments. The sites are all in the Mojave Desert/Great Basin weather patterns.

The data of Table 1 were used to compute the temperature parameters per equations 2 – 4; Table 2 summarizes the resulting parameters. Upon plotting, Figure 2 shows the scaling of T_a with altitude, in which the data show a high degree of correlation with the straight-line fit. Note that the slope is -1.8ºC/1000 feet, which agrees well with the mean adiabatic lapse rate of -1.9ºC/1000 feet. Figure 3 shows the corresponding plot for V_a, again exhibiting a relatively tight grouping. (Generally differences between measured quantities are less numerically stable then averages because of random fluctuations; in this case the parameter is a difference of averages, and it appears to be fairly stable and predictable.) On the other hand, the plot of V_d against altitude (Figure 4) shows very poor correlation. In this case the quantity V_d again represents a difference of measured quantities, so the instability is not unexpected; in addition, the data represent short-term phenomena, which tend to be less stable than long-term data.

Figures 2 – 4 also display the linear best fit equation for each case. For V_d, the very small value of R^2 suggests that the best strategy is not to scale at all, but to use the mean value, 15.8ºC, as the best estimate.

The data of Table 1 can also be used to examine microclimatic effects. Significant microclimatic differences exist between Inyokern and China Lake Armitage Field, which are within 15 km of each other and in the same valley. However, examination of the temperature parameter data in Table 2 suggests that such

microclimates have little effect on T_a and V_a, which both lie close to the best-fit curve (Figs. 2 and 3). The last parameter, V_d, does not track well between the two sites, but it is unstable anyway, as Figure 4 shows. Thus, if microclimatic effects are present, they will probably appear primarily in V_d, and even there it is not clear whether the differences are predictable.
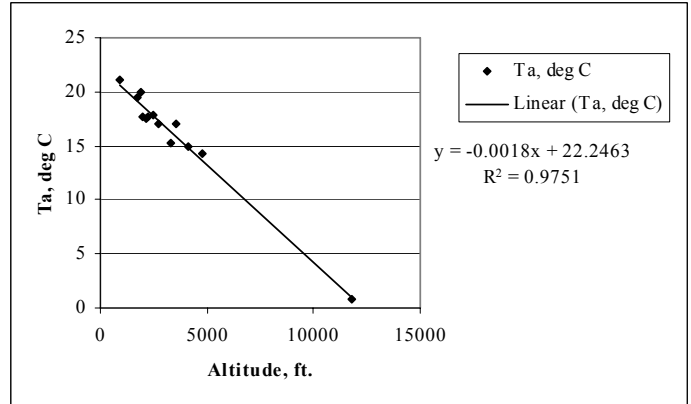

Figure 2. Scaling of average annual temperature with altitude, high desert sites.

Meteorological theory (e.g. Cole 1970) suggests that T_a should scale for altitude by the mean adiabatic lapse rate, as shown in Figure 2. Figure 3 shows a similar scaling for V_a, suggesting that T_a and V_a should be related, so that knowing T_a should allow predicting V_a. Figure 5 shows the strong correlation between T_a and V_a, which demonstrates that V_a can be predicted with considerable accuracy if T_a is known.
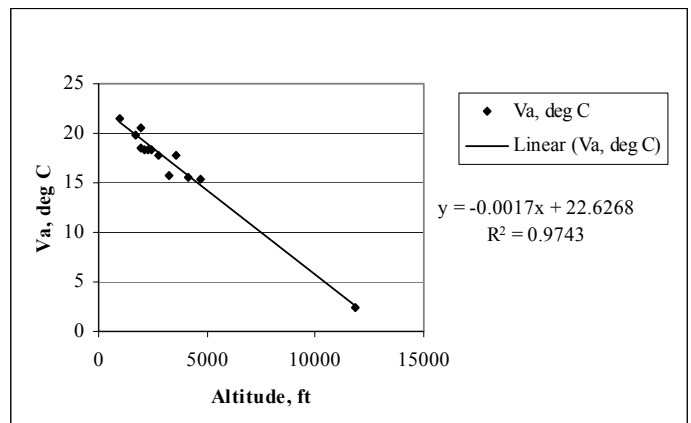

Figure 3. Scaling of annual temperature variation with altitude, high desert sites.

Table 2. Temperature parameters calculated for high desert sites.				
Station	**Alt, ft**	**Ta, deg C**	**Va, deg C**	**Vd, deg C**
Baker	940	21.17	21.56	17.67
Trona	1700	19.47	19.82	14.25
Daggett Apt	1930	20.03	20.61	15.17
Cantil	1960	17.67	18.51	18.08
Barstow	2140	17.47	18.31	17.89
China Lake Armitage Fld	2240	17.64	18.33	16.94
Inyokern	2440	17.86	18.32	18.31
Mojave	2740	17.06	17.81	14.56
Haiwee	3282	15.19	15.74	15.42
Randsburg	3570	17.00	17.74	13.25
Wildrose	4100	14.86	15.57	14.75
Mtn Pass	4740	14.36	15.29	13.53
WhiteMtn	11811	0.86	2.46	15.14

Thus, for this desert case the annual average temperature was shown to be predicted by the equation

$$T_a = 22.25 - 1.80x \quad (5)$$

where x is altitude in thousands of feet. The error standard deviation of this model is 0.79ºC, for the data set of Table 2. The annual temperature variation was found to decrease by 1.7ºC/1000 ft. altitude increase, and to be predicted by

$$V_a = 22.63 - 1.70x \quad (6)$$

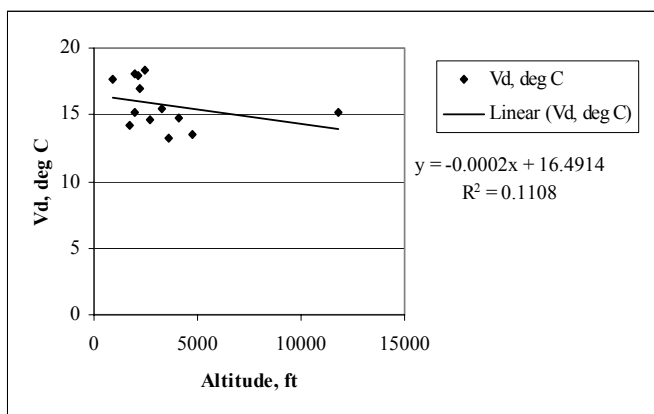with x defined as above. The error standard deviation is 0.76ºC.

Figure 4. Scaling of mean diurnal temperature variation, high desert sites.

As shown in Figure 4, the predictability of V_d with altitude is poor, so, in the absence of other data about a site, the most robust estimate is simply the mean:

$$V_d = 15.8ºC \quad (7)$$

with an error standard deviation of 1.79ºC. Finally, if T_a is known for a site, V_a is predicted by

$$V_a = 1.65 + 0.94T_a, \quad (8)$$
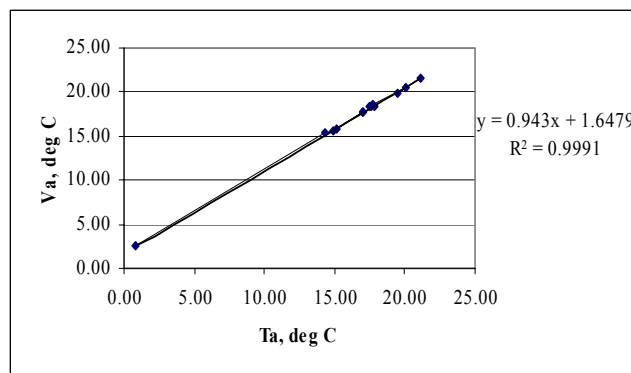
with an error standard deviation of 0.27ºC.

Figure 5. Correlation between annual average temperature and annual temperature variation, high desert sites.
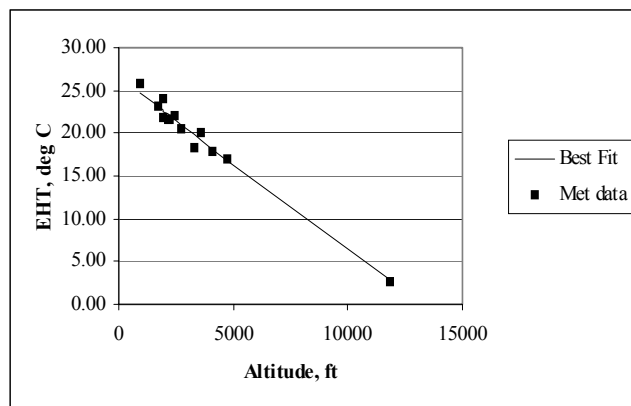
Figure 6. Effective hydration temperature for high desert sites as a function of altitude, showing comparison of computation from best fit data and meteorological data for each site.

The purpose of the parameters is computation of effective hydration temperature (EHT) by equation 1. Figure 6 shows the EHT computed from equation 1 with equations 5 – 7 as input,

Table 3. Temperature data for Central Valley sites.								
Station	Alt, ft	Ave Max, deg F	Ave Min, deg F	Annual Ave, deg F	Jul Max, deg F	Jul Min, deg F	Jan Max, deg F	Jan Min, deg F
Sacramento Airpt	20	73.8	48.5	61.2	92.3	58.2	53.9	38.9
Stockton	30	74.7	49.2	62.0	93.7	61.1	54.1	38.4
Lodi	40	74.2	46.6	60.4	90.9	56.3	55.0	37.6
Knights Ferry	320	74.0	45.8	59.9	94.3	58.9	53.5	35.0
Electra PH	700	75.8	44.5	60.2	96.5	55.9	57.2	34.1
New Melones Dam	780	74.8	44.9	59.9	95.5	58.5	55.2	33.0
Auburn	1360	71.8	48.8	60.3	91.2	62.4	54.4	37.2
Sonora	1830	73.2	42.5	57.9	93.9	56.0	55.8	31.9
Placerville	1890	71.7	44.4	58.1	91.2	57.5	55.0	33.3
Grass Valley	2400	68.4	42.1	55.3	86.5	55.0	53.9	31.8
Nevada Cty	2600	66.9	42.6	54.8	86.4	56.0	50.7	32.3
Deer Cr PH	3700	61.6	36.4	49.0	82.8	47.0	41.1	27.4

labeled "Best Fit"; it also shows EHT computed from equation 1 using the site meteorological data as inputs, labeled "Met data". The error standard deviation of the between the two EHT estimates is 0.82°C. This accuracy is surprising because of the relatively large error in V_d; however, inspection of equation 1 shows that this arises because the EHT computation is dominated by the T_a value, which is characterized by smaller errors than V_d. The agreement between the two methods is remarkable.

Figure 7. Scaling of average annual temperature with altitude, Central Valley sites. Note break around 1500 ft.

Central Valley

The western slope of the Sierra Nevada presents a different case, in which less vertical relief exists and climate is dominated by a persistent temperature inversion layer in the Central Valley. The analysis is again based on monthly temperature data from the Western Regional Climate Center (WRCC), using the data base from 1971 – 2000. Table 3 summarizes the sites used in the temperature scaling analysis. All are in similar weather patterns. Temperature parameters were again computed by equations 2 – 4, and Table 4 summarizes the parameters.
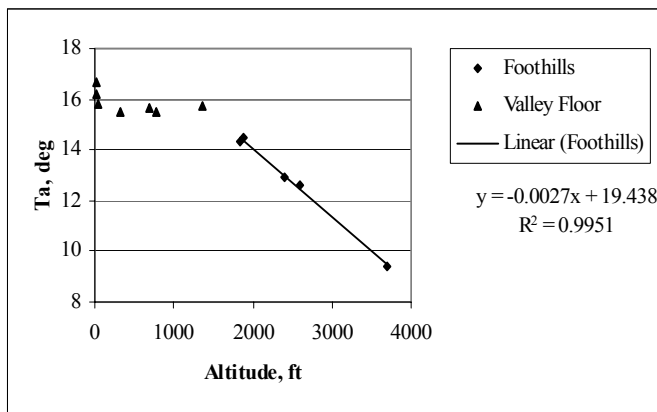

Figure 8. Scaling of annual temperature variation with altitude, Central Valley sites.

Figure 7 shows the variation of T_a with altitude. As can be seen, the data for this case fall into two distinct patterns: valley floor and lower foothills, and higher foothills and mountains. The break point between the two is approximately 1500 feet altitude, probably correlating with the level of the normal inversion layer over the valley. Below this altitude, T_a is roughly independent of

altitude, and has an average value of 15.85°C. Above 1500 ft the value of T_a is given by

$$T_a = 19.44 - 2.7x, \quad 1500 < x < 4000 \quad (9)$$

where x is altitude in thousands of feet.

Figure 8 shows the similar plot for V_a, again exhibiting a break at about 1500 ft. The average value of Va below 1500 ft is 16.02°C, while above 1500 ft the value is

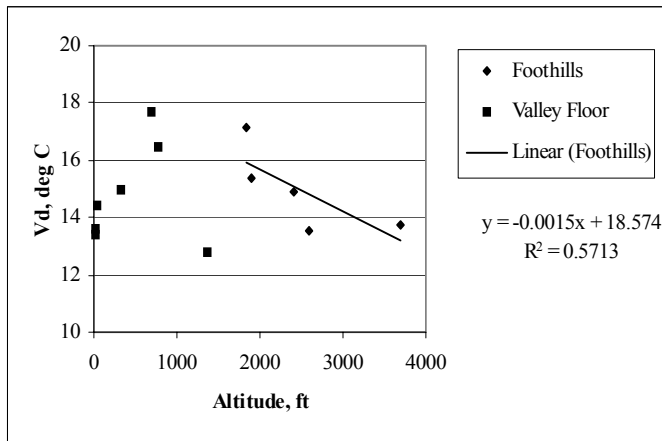$$V_a = 20.75 - 2.9x, \quad 1500 < x < 4000 \quad (10)$$

Figure 9. Scaling of mean diurnal temperature variation with altitude, Central Valley sites.

Finally, Figure 9 shows the scaling for V_d, with much poorer correlation with altitude, but noticeably better than the fit for the desert case. Analysis of accuracy shows that use of the altitude scaling gives better results than simply using the average, as was done for the desert. Thus, for sites below 1500 ft, the best fit is the mean value of V_d is 14.77°C; above that altitude the best fit is

$$V_d = 18.57 - 1.5x, \quad 1500 < x < 4000 \quad (11)$$

Figure 7 and Figure 8 again show similar scaling with altitude for T_a and V_a, and Figure 10 shows that there is again strong correlation between T_a and V_a. However, there is a different grouping for valley floor and foothills, except this time the break point is below 100 ft. The equation relating T_a and V_a is

$$V_a = 1.21T_a - 3.57, 0 < x < 100 \quad (12a)$$

$$V_a = 0.83T_a + 3.03, \quad 100 < x < 4000 \quad (12b)$$

Since the best fit to the data shows a break point, assessing parameter accuracy is more complex than for the desert case. Table 5 summarizes the accuracy achieved by this method, including a computation for effective hydration temperature made using equation 1. It can be seen that the algorithms yield values of T_a and V_a which are within 0.5°C, and V_d within 1.7°C. Surprisingly, in view of the possible errors in V_d, the EHT values are within 0.5°C, again because the EHT computation is dominated by the T_a value, which is characterized by the smallest errors.
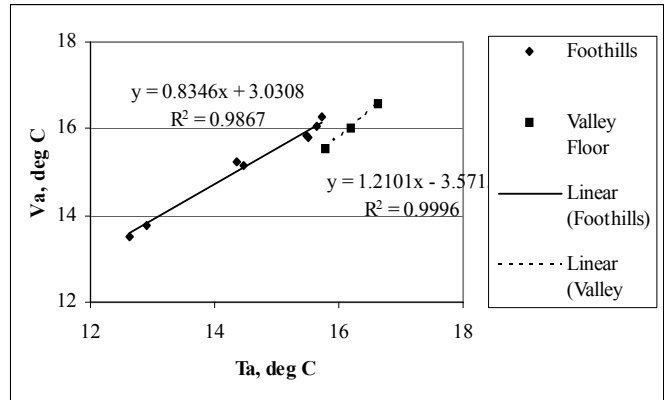

Figure 10. Correlation of average annual temperature with annual temperature variation, Central Valley sites. The break point is at approximately 100 ft altitude.
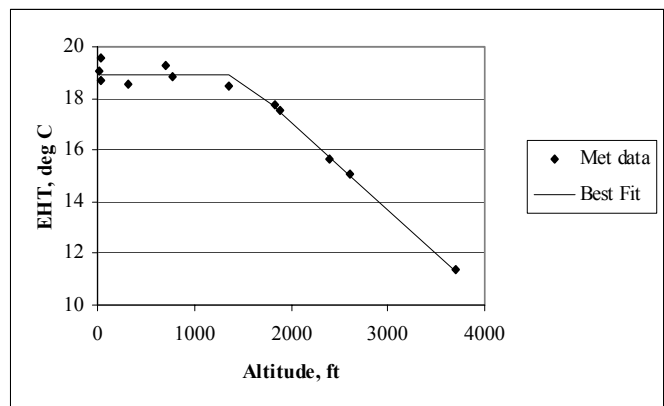

Figure 11. Effective hydration temperature for desert sites as a function of altitude, showing comparison of computation from best fit data and meteorological data for each site. Central Valley conditions.

Table 4. Computed temperature parameters for Central Valley sites.				
Station	**Alt, ft**	**Ta, deg C**	**Va, deg C**	**Vd, deg C**
Sacramento Airpt	20	16.19	16.01	13.64
Stockton	30	16.64	16.57	13.42
Lodi	40	15.78	15.53	14.44
Knights Ferry	320	15.50	15.79	14.97
Electra PH	700	15.64	16.07	17.69
New Melones Dam	780	15.47	15.86	16.44
Auburn	1360	15.72	16.28	12.78
Sonora	1830	14.36	15.22	17.17
Placerville	1890	14.47	15.14	15.39
Grass Valley	2400	12.92	13.78	14.89
Nevada Cty	2600	12.64	13.53	13.56
Deer Cr PH	3700	9.44	9.76	13.75

Figure 11 shows the values of EHT for the Central Valley sites, again computed from equation 1 with two different inputs. The solid line shows the values computed using the temperature model as summarized in Table 5, and the points show the EHT computed from the meteorological data for each site from Table 4. The agreement is obviously good.

The foregoing analysis suggests that for sites below approximately 1500 ft the best estimate of the temperature parameters is the mean for the site ensemble; above that altitude, altitude scaling should be employed.

Discussions and Conclusions

The two case studies summarized above show that the form of the algorithm providing the best fit can only be determined from examination of the data, in conjunction with the physics of weather patterns, and may be different in different climatic regions. Judgment is required in doing this, and it is not possible to predict in advance what the best form of the temperature algorithms will be.

The method which gave the best results for high desert conditions was not the same as the best for the Central Valley conditions. In the desert, T_a and V_a scaled very accurately with altitude, while V_d was best estimated by a mean value independent of altitude. In the Central Valley, none of the parameters for the sites below 1500 ft scaled with altitude, although altitude scaling was effective from 1500 – 4000 ft. A second difference was that, for the Central Valley sites, mean diurnal variation above 1500 ft has a positive correlation with altitude, so that use of altitude scaling yielded better accuracy in EHT than use of the mean.

The rates of decline of T_a and V_a with altitude varied as well between the two cases. In the desert, both approximated the mean adiabatic lapse rate, while in the Central Valley the rate of decrease with altitude above 1500 ft is much larger (-2.7°C/1000 ft for T_a and -2.9°C/1000 ft for V_a). This more rapid decrease may be due to a sharp decline in humidity above the inversion layer, a phenomenon which does not occur in the desert.

Table 5. Analysis of accuracy of temperature parameter models.				
Parameter	**Site Altitude, ft.**	**Algorithm for Estimate, deg C**	**Mean Error, deg C**	**Error StDev, deg C**
Ta	< 1500	15.85	0.00	0.42
	> 1500	Ta = 19.44 - 0.0027x	0.02	0.14
	Overall	-	0.01	0.32
Va	< 1500	16.02	0.00	0.34
	> 1500	Va = 20.75 - 0.0029x	-0.06	0.23
	Overall	-	-0.03	0.29
Vd	< 1500	14.77	0.00	1.67
	> 1500	Vd = 18.57 - 0.0015x	0.11	0.95
	Overall	-	0.04	1.42
EHT	< 1500	Equation 1a,b	0.02	0.40
	> 1500	Equation 1a,b	0.04	0.06
	Overall	Equation 1a,b	0.02	0.29

A final observation involves limits of validity of the resulting algorithms. First, the effects of paleoclimatic change have not been included; an implicit assumption was made that the parameters representing current temperature conditions are also valid through time. It is known that climatic shifts have occurred (West et al. 2007), but the effects of such shifts on obsidian hydration are generally small, < 7% in age (Rogers 2007b). A method for accounting for them has been described elsewhere (Rogers 2007b). Further, the algorithms for each case study were developed based on regions which are limited in geographical extent, in altitude, and in extent of general weather patterns. The algorithms should not be applied outside those limits without further analyses to verify validity - extrapolation is always dangerous.

In summary, regional analysis of temperature, based on publicly-available meteorological data, can yield valid algorithms for estimating temperature parameters at an archaeological site in the region. If an archaeological site is located in close proximity to a current weather station, the 30-year climate data from the station can be used to calculate the temperature parameters; otherwise, a regional temperature analysis should be performed as exemplified by the case studies in this paper. The resulting temperature parameters are representative of long-term present weather conditions, and provide the basis for accurate computations of effective hydration temperature in support of chronological analyses.

References

Carslaw, H. S., and J. C. Jaeger
1959 *Conduction of Heat in Solids*, 2nd ed. Clarendon Press, Oxford.

Cole, F. W.
1970 *Introduction to Meteorology.* Wiley, New York.

Everett-Curran, L., R. G. Milo, and D. Quiatt
1991 Microgeographic Comparisons of Climate Today Afford Inferences Concerning Past Behavior: An Overview of Data and Applications from a Study of Chapin Mesa Climate. In *Anasazi Symposium 1991*, A. Hutchinson and J. E. Smith (eds.), pp. 109-116. Mesa Verde Museum Association.

Friedman, I., and W. Long
1976 Hydration Rate of Obsidian. *Science* 191(1):347-352.

Gilreath, A. J., and W. R. Hildebrandt
1997 *Prehistoric Use of the Coso Volcanic Field.* No. 56, Contributions of the University of California Archaeological Research Facility. Berkeley.

Johnson, M. J., C. J. Mayers, and B. J. Andraski
2002 *Selected Micrometeorological and Soil-Moisture Data at Amargosa Desert Research Site in Nye County near Beatty, Nevada, 1998 – 2000.* U.S. Geological Survey Open-File Report 02-348. USGS, Carson City, Nevada.

Rogers, A. K.
2007a Effective Hydration Temperature of Obsidian: A Diffusion-Theory Analysis of Time-Dependent Hydration Rates. *Journal of Archaeological Science.* 34:656-665.
2007b *How Did the Altithermal Affect Obsidian Hydration Rates? A Model-Based Study of the Hydration Process and Paleoclimatic Change.* Paper presented at the 2nd Three-Corners Conference, Las Vegas, NV.
2008 Field Data Validation of an Algorithm for Computing Obsidian Effective Hydration Temperature. *Journal of Archaeological* Science 35:441-447.

Stevenson, C. M., J. Carpenter, and B. E. Scheetz
1989 Obsidian Dating: Recent Advances in the Experimental Determination and Application of Hydration Rates. *Archaeometry* 31(2):1193-1206.

Stevenson, C. M., J. J. Mazer, and B. E. Scheetz
1998 Laboratory Obsidian Hydration Rates: Theory, Method, and Application. In *Archaeological Obsidian Studies: Method and Theory. Advances in Archaeological and Museum Science*, Vol. 3, M. S. Shackley (ed.), pp.181-204. Plenum Press, New York.

Stevenson, C. M., M. Gottesman, and M. Macko
2000 Redefining the Working Assumptions for Obsidian Hydration Dating. *Journal of California and Great Basin Anthropology* 22(2):223-236.

Stevenson, C. M., I. M. Abdelrehim, and S. W. Novak
2004 High Precision Measurement of Obsidian Hydration Layers on Artifacts from the Hopewell Site Using Secondary Ion Mass Spectrometry. *American Antiquity* 69(4):555-568.

West, G. J., W. Woolfenden, J. A. Wanket, and R. S. Anderson
2007 Late Pleistocene and Holocene Environments. In *California Prehistory: Colonization, Culture, and Complexity*, T. L. Jones and K. A. Klar (eds.), pp. 11-34. Altamira Press, Walnut Creek.

ABOUT OUR WEB SITE

The IAOS maintains a website at http://www.peak.org/obsidian/
The site has some great resources available to the public, and our webmaster, Craig Skinner, continues to update the list of publications and must-have volumes.

NEW: You can now become a member online or renew your current IAOS membership using PayPal. Please take advantage of this opportunity to continue your support of the IAOS.

Other items on our website include:

- World obsidian source catalog
- Back issues of the *Bulletin.*
- An obsidian bibliography
- An obsidian laboratory directory
- Photos and maps of some source locations
- Links

Thanks to Craig Skinner for maintaining the website. Please check it out!

CALL FOR ARTICLES

Submissions of articles, short reports, abstracts, or announcements for inclusion in the *Bulletin* are always welcome. We accept electronic media on IBM compatible disks and CD in a variety of word processing formats, but MS Word or WordPerfect are preferred. Files can also be emailed to the *Bulletin* at cdillian@princeton.edu Please include the phrase "IAOS Bulletin" in the subject line. An acknowledgement email will be sent in reply, so if you do not hear from us, please email again and inquire.

Deadline for Issue #40 is November 1, 2008.

Send submissions to:

Carolyn Dillian
IAOS *Bulletin* Editor
c/o Princeton University
Princeton Writing Program
Whitman College
South Baker Hall
Princeton, NJ 08544
U.S.A.

Inquiries, suggestions, and comments about the *Bulletin* can be sent to cdillian@princeton.edu Please send updated address information to Colby Phillips at colbyp@u.washington.edu

MEMBERSHIP

The IAOS needs membership to ensure success of the organization. To be included as a member and receive all of the benefits thereof, you may apply for membership in one of the following categories:

Regular Member: $20/year*
Institutional Member: $50/year
Student Member: $10/year or FREE with submission of a paper to the *Bulletin* for publication. Please provide copy of current student identification.
Lifetime Member: $200

Regular Members are individuals or institutions who are interested in obsidian studies, and who wish to support the goals of the IAOS. Regular members will receive any general mailings; announcements of meetings, conferences, and symposia; the *Bulletin*; and papers distributed by the IAOS during the year. Regular members are entitled to vote for officers.

Institutional Members are those individuals, facilities, and institutions who are active in obsidian studies and wish to participate in interlaboratory comparisons and standardization. If an institution joins, all members of that institution are listed as IAOS members, although they will receive only one mailing per institution. Institutional Members will receive assistance from, or be able to collaborate with, other institutional members. Institutional Members are automatically on the Executive Board, and as such

have greater influence on the goals and activities of the IAOS.

*Membership fees may be reduced and/or waived in cases of financial hardship or difficulty in paying in foreign currency. Please complete the form and return it to the Secretary-Treasurer with a short explanation regarding lack of payment.

NOTE: Because membership fees are very low, the IAOS asks that all payments be made in U.S. Dollars, in international money orders, or checks payable on a bank with a U.S. branch. Otherwise, please use PayPal on our website to pay with a credit card. http://www.peak.org/obsidian/

For more information about the IAOS, contact our Secretary-Treasurer:

Colby Phillips
IAOS
c/o University of Washington
Department of Anthropology
Box 353100
Seattle, WA 98195-3100
U.S.A.
colbyp@u.washington.edu

Membership inquiries, address changes, or payment questions can also be emailed to colbyp@u.washington.edu

---

ABOUT THE IAOS

The International Association for Obsidian Studies (IAOS) was formed in 1989 to provide a forum for obsidian researchers throughout the world. Major interest areas include: obsidian hydration dating, obsidian and materials characterization ("sourcing"), geoarchaeological obsidian studies, obsidian and lithic technology, and the prehistoric procurement and utilization of obsidian. In addition to disseminating information about advances in obsidian research to archaeologists and other interested parties, the IAOS was also established to:

1. Develop standards for analytic procedures and ensure inter-laboratory comparability.
2. Develop standards for recording and reporting obsidian hydration and characterization results
3. Provide technical support in the form of training and workshops for those wanting to develop their expertise in the field
4. Provide a central source of information regarding the advances in obsidian studies and the analytic capabilities of various laboratories and institutions.

MEMBERSHIP RENEWAL FORM

We hope you will continue your membership. Please complete the renewal form below.

NOTE: You can now renew your IAOS membership online! Please go to the IAOS website at http://www.peak.org/obsidian/ and check it out! Please note that due to changes in the membership calendar, your renewal will be for the next calendar year. Unless you specify, the *Bulletin* will be sent to you as a link to a .pdf available on the IAOS website.

___ Yes, I'd like to renew my membership. A check or money order for the annual membership fee is enclosed (see below).

___ Yes, I'd like to become a new member of the IAOS. A check or money order for the annual membership fee is enclosed (see below). Please send my first issue of the IAOS *Bulletin*.

___ Yes, I'd like to become a student member of the IAOS. I have enclosed either an obsidian-related article for publication in the IAOS *Bulletin* or an abstract of such an article published elsewhere. I have also enclosed a copy of my current student ID. Please send my first issue of the IAOS *Bulletin*.

NAME: _____

TITLE: _____ AFFILIATION:_____

STREET ADDRESS: _____

CITY, STATE, ZIP: _____

COUNTRY: _____

WORK PHONE: _____ FAX: _____

HOME PHONE (OPTIONAL): _____

EMAIL ADDRESS: _____

My check or money order is enclosed for the following amount (please check one):
___ $20 Regular
___ $10 Student (include copy of student ID)
___ FREE Student (include copy of article for *Bulletin* and student ID)
___ $50 Institutional
___ $200 Lifetime

Please return this form with payment to:
Colby Phillips
IAOS
c/o University of Washington
Department of Anthropology
Box 353100
Seattle, WA 98195-3100
U.S.A.